JOURNAL OF MATERIALS SCIENCE 37 (2002) 1155–1163

Effects of interface structures on cracking in AlN(11$\bar{2}$0)/α-Al_2O_3(1$\bar{1}$02) epitaxial films

K. KAIGAWA*, T. SHIBATA, Y. NAKAMURA, K. ASAI, M. TANAKA, H. SAKAI
NGK Insulators, Ltd., 2-56 Suda-cho, Mizuho-ku, Nagoya 467-8530, Japan
E-mail: kaigawa@ngk.co.jp

T. TSURUMI
Department of Metallurgy & Ceramics Science, Graduate School of Science & Engineering, Tokyo Institute of Technology, 2-12-1 Ookayama, Meguro-ku, Tokyo 152-8552, Japan

The crystal structures and microstructures of AlN(11$\bar{2}$0)/GaN(11$\bar{2}$0) epitaxial films on just-cut and ±4° off-cut Al_2O_3(1$\bar{1}$02) substrates grown by metal organic chemical vapor deposition (MOCVD) are investigated using high-resolution X-ray diffractometry and transmission electron microscopy, and are compared with those of AlN(11$\bar{2}$0) film on +4° off-cut Al_2O_3(1$\bar{1}$02) substrate. In the AlN/Al_2O_3(+4° off-cut) film and the AlN/GaN/Al_2O_3 (just-cut, −4° off-cut) films, cracks parallel to the $[1\bar{1}00]_{AlN}$ direction and perpendicular to the interfaces of the films and the substrates are observed. The AlN/Al_2O_3 and AlN/GaN interfaces exhibit low crystallinity in which moiré fringes are observed. On the other hand, in the AlN/GaN/Al_2O_3(+4° off-cut) film, no cracks form. The GaN layer buffers the lattice mismatch between the AlN film and the Al_2O_3 substrate, and moiré fringes are not observed in the GaN/Al_2O_3 and AlN/GaN interfaces. On the basis of these results, the effects of the interface structures on cracking are discussed.

1. Introduction

AlN(11$\bar{2}$0)/α-Al_2O_3(1$\bar{1}$02) heteroepitaxial films, which have the $[0001]_{AlN}//[1\bar{1}01]_{Al2O3}$ and $[1\bar{1}00]_{AlN}//[11\bar{2}0]_{Al2O3}$ orientation relationship between AlN films and Al_2O_3 substrates, have been proposed as a piezoelectric material for GHz surface acoustic wave (SAW) devices for applications in wireless communication systems, because of its high SAW velocity (5910 m/s), moderate electromechanical coupling coefficient (∼1.0%), and zero temperature coefficient of delay (TCD) [1–6]. AlN films thicker than 2 μm are required in order to obtain the physical properties required for use in SAW devices. However, cracks propagate in AlN/Al_2O_3 films when the films become thicker than about 1 μm. Several studies on the cracking mechanism in nitride epitaxial films were carried out [2–4, 7–12]. Duffy *et al.* reported that strain in the AlN(11$\bar{2}$0)/α-Al_2O_3(1$\bar{1}$02) film was anisotropic, because of differences in the elastic and thermal expansion properties of both film and substrate with respect to their different crystallographic directions [2]. Yim *et al.* reported that cracks in the AlN/Al_2O_3 epitaxial films were explained by thermal stress, based on the fact that cracking could be eliminated by slowly cooling the specimen [3]. In GaN(0001)/Al_2O_3(0001) heteroepitaxial films, Matsumoto *et al.* [7], Itoh *et al.* [8] and Hiramatsu *et al.* [9] measured curvature after cooling, observed cross-sectional microstructures, and discussed dependencies of lattice constants on film thickness. As the results, they concluded that the cracks were formed by thermal stress due to difference in thermal expansion coefficients between GaN and Al_2O_3. On the other hand, Amano *et al.* [10] and Dobrynin [11] found that tensile stress was induced in the GaN(0001)/Al_2O_3(0001) and AlN(11$\bar{2}$0)/Al_2O_3(1$\bar{1}$02) heteroepitaxial films during the growth by *in situ* curvature measurements. Dobrynin concluded that the cracks were formed by tensile stress during the epitaxial growth. Despite of these studies, the cracking mechanism in the AlN(11$\bar{2}$0)/Al_2O_3(1$\bar{1}$02) heteroepitaxial films has not yet been understood fully. The lack of the fundamental understanding hinders the development of the films. Recently, we reported that cracks in the AlN(11$\bar{2}$0)/Al_2O_3(1$\bar{1}$02) films were formed in the film due to tensile stress along the $[0001]_{AlN}$ direction during epitaxial growth, based on the analyses of the crystal structures and the cross-sectional microstructures [12]. On the other hand, no cracks formed in the AlN/GaN/Al_2O_3(+4° off-cut) film with the GaN layer, but the role of the GaN layer could not be clarified.

In this study, we further investigated the crystal structures and microstructures of the AlN(11$\bar{2}$0) film on a +4° off-cut Al_2O_3(1$\bar{1}$02) substrate and

*Author to whom all correspondence should be addressed.

the AlN(11$\bar{2}$0)/GaN(11$\bar{2}$0) heteroepitaxial films on just-cut and ±4° off-cut Al_2O_3(1$\bar{1}$02) substrates using high-resolution X-ray diffractometry (HR-XRD), and a transmission electron microscope (TEM). On the basis of the results, the effects of the interface structures on cracking are discussed.

2. Experimental procedure

2.1. Film growth

AlN and AlN/GaN epitaxial films were grown on 3-inch-diameter α-Al_2O_3(1$\bar{1}$02) substrates 430 μm thick by metal organic chemical vapor deposition (MOCVD). Just-cut and ±4° off-cut α-Al_2O_3 wafers were used as the substrates. In the case of the conventional wafer (just-cut), the interfacial angle between the surface, which is the (1$\bar{1}$02) plane, and the (0001) planes is 57.6°. In the case of the off-cut wafers, the surfaces are tilted slightly from the (1$\bar{1}$02) planes, and the interfacial angle of the +4° off-cut wafer between the surface and the (0001) plane is 61.6° (=57.6 + 4), whereas the interface angle of the −4° off-cut wafer is 53.6° (=57.6 − 4). In this study, AlN/Al_2O_3 (+4° off-cut) film and AlN/GaN/Al_2O_3 (just-cut, ±4° off-cut) films were grown. Since the details of sample preparation were reported in previous papers [6, 12], only a brief outline is described below. The substrate was first annealed in H_2 ambient, and then the initial nitriding layer was formed by heating the substrate at 1100°C in a flow of mixed NH_3 and H_2 in a horizontal reactor. Subsequently, trimethylaluminum (TMA, $(CH_3)_3Al$) was introduced into the reactor to grow AlN epitaxial film at 15–20 Torr. In the case of the AlN/GaN/Al_2O_3 film, trimethylgallium (TMG, $(CH_3)_3Ga$) was introduced into the reactor after the first annealing process to grow the GaN layer (∼0.2 μm) at 15 Torr for 10 min.

2.2. Crystal structure analysis

The crystallinity and crystal structures of the AlN films and GaN layers were characterized using HR-XRD (Philips, MRD) with a two-crystal, four-reflection Bartels monochromator [13] as incident optics and a one-crystal, two-reflection analyzer as diffracted optics. The monochromator and analyzer crystals were made from perfect Ge crystals, and were set to reflect from the (220) planes using Cu $K_{\alpha 1}$ radiation. The ω-scan

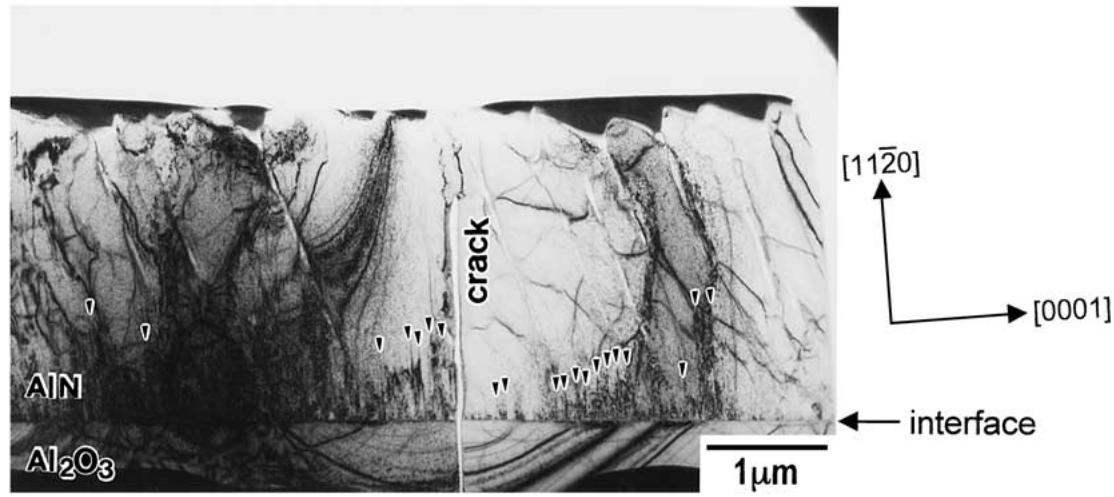

(a)

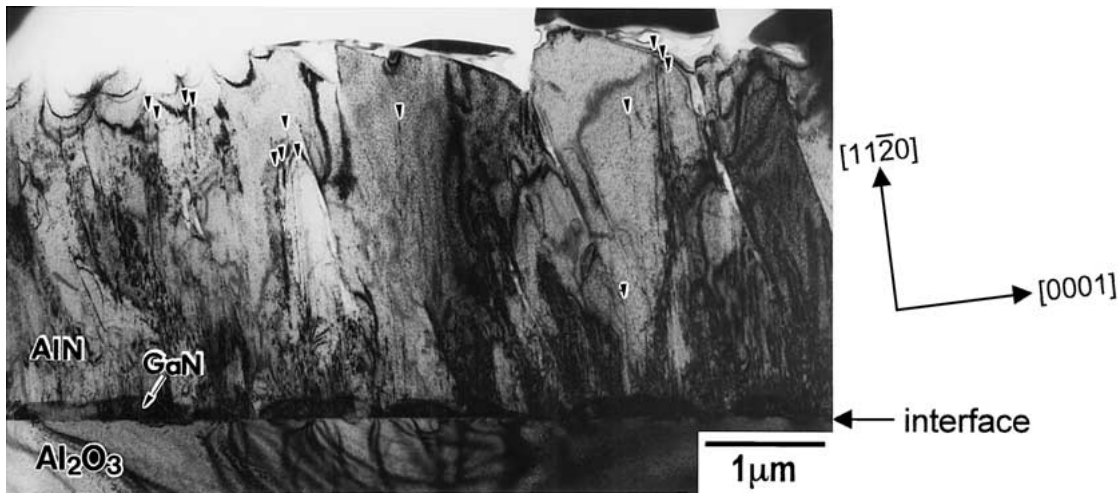

(b)

Figure 1 AlN (1$\bar{1}$00) cross-sectional bright-field TEM images of (a) the AlN/Al_2O_3(+4° off-cut) film, (b) the AlN/GaN/Al_2O_3(+4° off-cut) film, (c) the AlN/GaN/Al_2O_3(just-cut) film, and (d) the AlN/GaN/Al_2O_3(−4° off-cut) film. Symbols (▼) indicate the planar imperfections induced along the $(0001)_{AlN}$ plane. (*Continued.*)

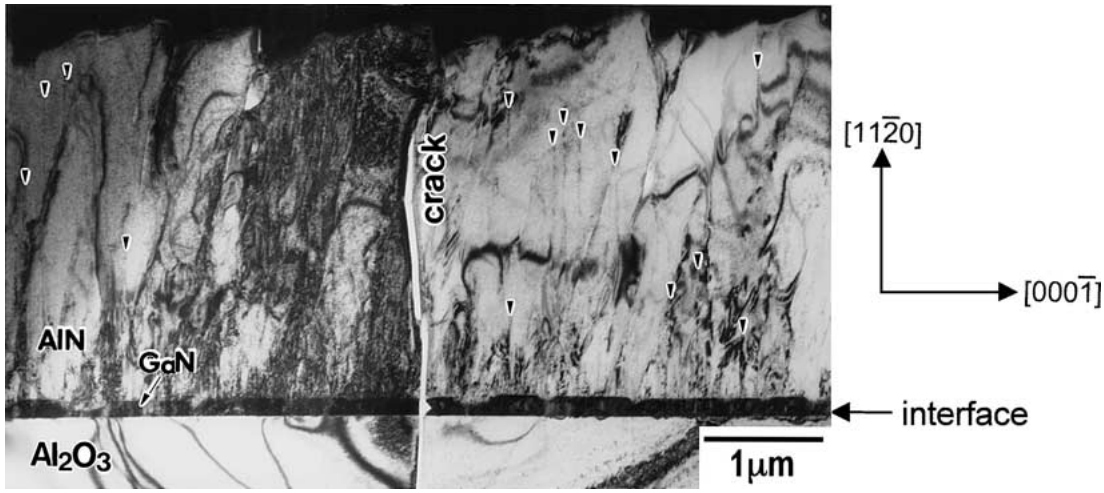

(c)

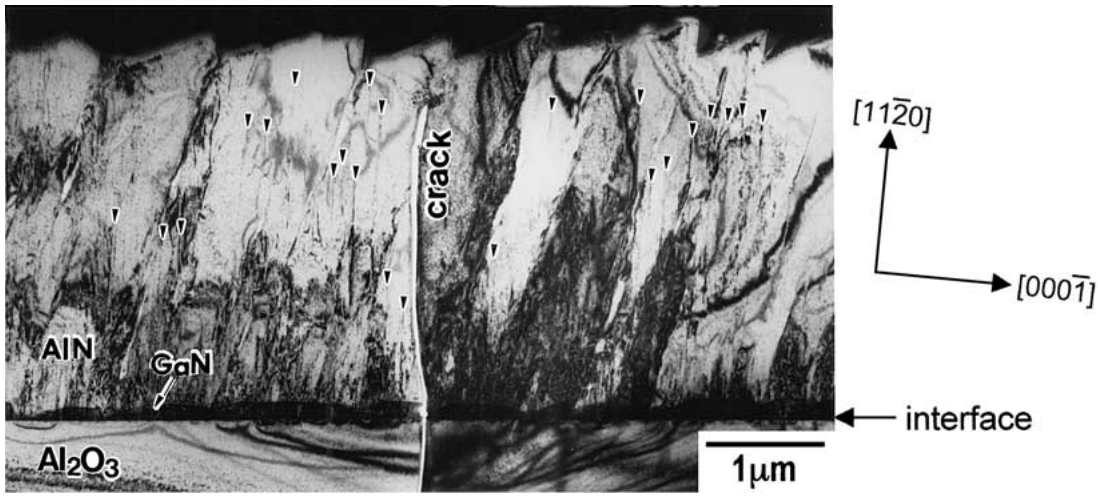

(d)

Figure 1 (*Continued.*)

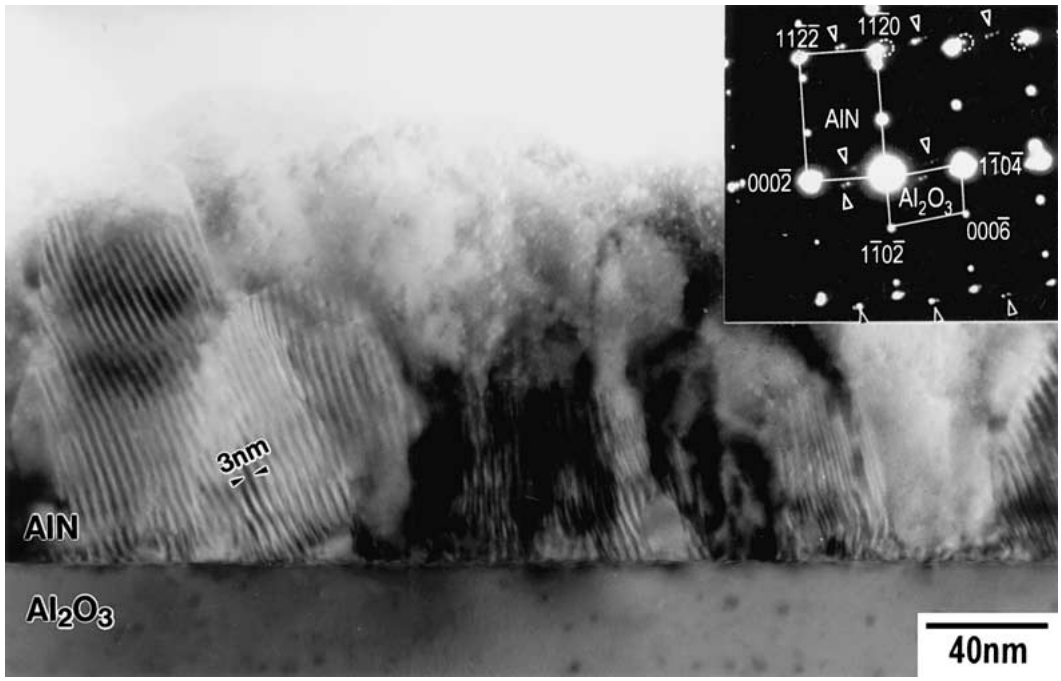

Figure 2 AlN (1$\bar{1}$00) cross-sectional TEM images of the AlN/Al_2O_3(+4° off-cut) film. Selected-area electron diffraction pattern at the top right of micrograph was obtained in the vicinity of the AlN/Al_2O_3 interface. Symbols (▲, ▼ and ○) indicate extra electron diffraction spots other than those of the AlN epitaxial film and the Al_2O_3 substrate.

rocking curves close to the $11\bar{2}0$ reflection of the AlN films and GaN layers were measured by aligning the $[0001]_{AlN}$ directions horizontal to the incident X-ray beam. The absolute lattice constants of AlN films and α-Al_2O_3 substrates were measured by the Fewster-Andrew method [14]. Additionally, the lattice constants of GaN layers were estimated from the peak mismatches of $\omega/2\theta$-scan rocking curves between the AlN films and GaN layers.

2.3. Microstructure observation

The cross-sectional AlN($1\bar{1}00$) images were obtained using a TEM operated at 200 kV (JEOL, JEM-2010). Ultra thin samples for TEM observations were prepared by either Ga ion beam sputtering at a voltage of 30 kV (FEI, FIB200) or Ar ion beam sputtering at a voltage of 4 kV (GATAN, Dual Ion Mill M-600).

3. Results and discussion

3.1. Crystal structures

3.1.1. Crystallinity

Table I shows the full-width at half maximum (FWHM) of the ω-scan X-ray rocking curves close to the $11\bar{2}0$ reflection of the AlN and the GaN. The FWHM corresponds to the degree of mosaic structure formation rather than the fluctuation in the lattice constant [12].

TABLE I Full-width at half maximum (FWHM) of the ω-scan X-ray rocking curves close to the $1\,1\,\bar{2}\,0$ reflection of AlN and GaN

Film system substrate	AlN/Al_2O_3	$AlN/GaN/Al_2O_3$		
	$+4^\circ$ off-cut	$+4^\circ$ off-cut	just-cut	-4° off-cut
AlN (minutes)	15.2	31.3	25.9	24.2
GaN (minutes)		55.8	56.7	68.7

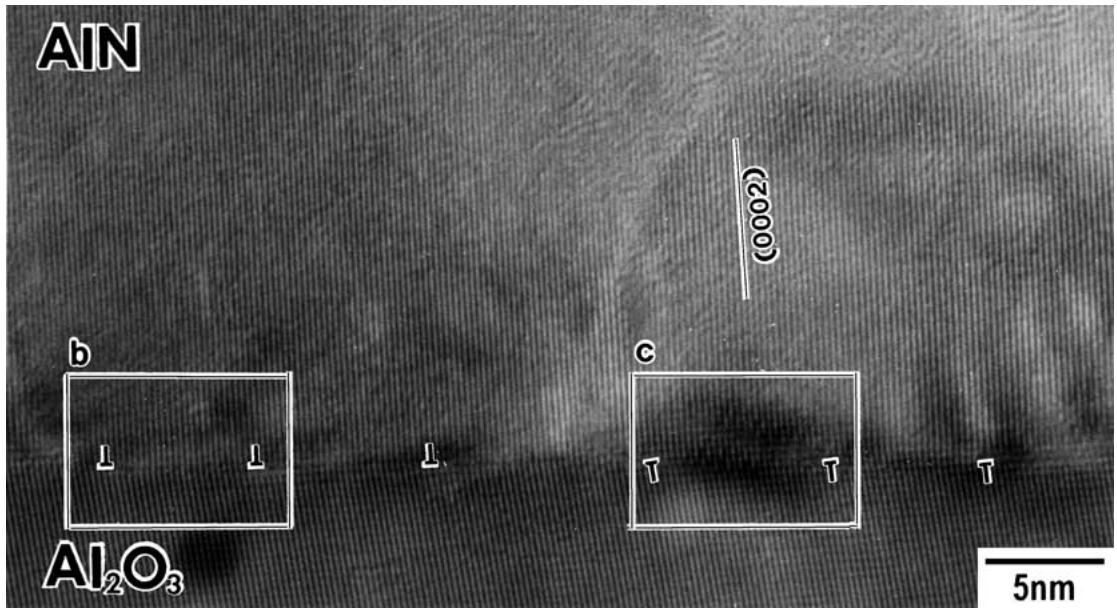

(a)

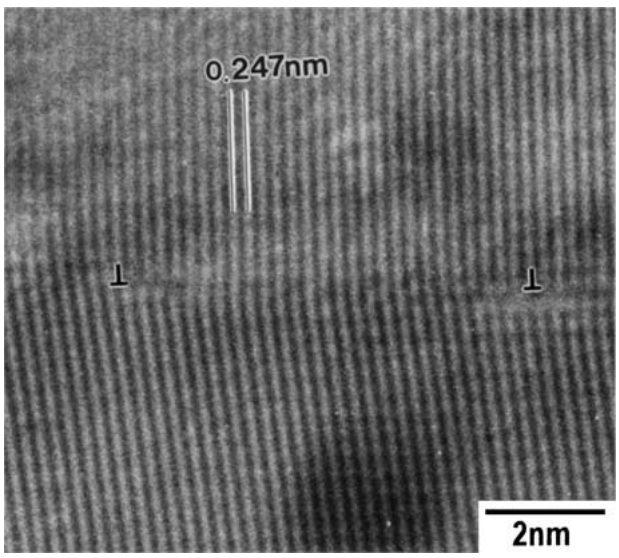

(b)

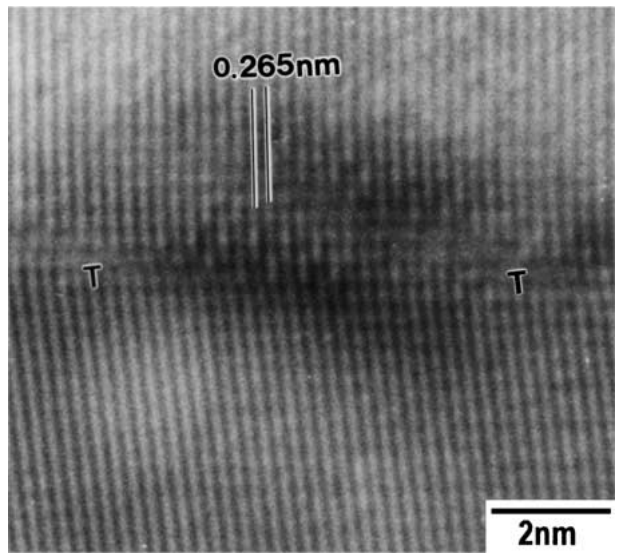

(c)

Figure 3 (a) AlN ($1\bar{1}00$) cross-sectional high-resolution TEM images of the AlN/Al_2O_3($+4^\circ$ off-cut) film. Enlarged images at the (b) left-hand and (c) right-hand sides of the micrograph (a). Misfit dislocations are labeled $\perp$ or $\top$.

TABLE II Interplanar spacings (d-spacings) of the AlN films, the GaN layers and the Al_2O_3 substrates along the $[0001]_{AlN}$ direction

Film system substrate	AlN/Al_2O_3 +4° off-cut	$AlN/GaN/Al_2O_3$ +4° off-cut	$AlN/GaN/Al_2O_3$ just-cut	$AlN/GaN/Al_2O_3$ −4° off-cut	JCPDS
$(0002)_{AlN}$ (nm)	0.2492	0.2489	0.2489	0.2490	0.24896
$(0002)_{GaN}$ (nm)		0.2556	0.2578	0.2575	0.2589
$(1\bar{1}0\bar{4})^{a}_{Al2O3}$ (nm)	0.2564	0.2564	0.2564	0.2564	0.25644

[a]The d-spacing of $(1\bar{1}0\bar{4})_{Al2O3}$ was converted into that parallel to the $[0001]_{AlN}$ direction.

The value of FWHM for the AlN in the AlN/Al_2O_3(+4° off-cut) film is half of those in the $AlN/GaN/Al_2O_3$ films. In the $AlN/GaN/Al_2O_3$ films, the values of FWHM for GaN are far larger than those for AlN. As the off-cut angle of the substrate increases, the values of FWHM for AlN increase, whereas those for GaN decrease. Thus, AlN in the $AlN/GaN/Al_2O_3$(+4° off-cut) film exhibits the lowest crystallinity, and that in the AlN/Al_2O_3(+4° off-cut) film exhibits the highest, among the four samples.

3.1.2. Lattice mismatch

Table II shows the interplanar spacings (d-spacings) along the $[0001]_{AlN,GaN}$ direction measured by HR-XRD. The data on the JCPDS cards (No.25-1133, 2-1078, 42-1468) are also shown. The d-spacing of $(1\bar{1}0\bar{4})_{Al2O3}$ is converted into that parallel to the $[0001]_{AlN}$ direction. In the AlN/Al_2O_3(+4° off-cut) and the $AlN/GaN/Al_2O_3$(just-cut, −4° off-cut) films, the d-spacings of $(0002)_{AlN}$ and $(0002)_{GaN}$ almost agree with the data on the JCPDS cards. The lattice mismatch of the AlN/Al_2O_3 interface in the AlN/Al_2O_3 (+4° off-cut) film is estimated to be −2.8%. The d-spacings of $(0002)_{GaN}$ are larger than those of $(0002)_{AlN}$ and $(1\bar{1}0\bar{4})_{Al2O3}$, and the lattice mismatches of the AlN/GaN and GaN/Al_2O_3 interfaces are estimated to be −3.4% and +0.5%, respectively. On the other hand, in the $AlN/GaN/Al_2O_3$(+4° off-cut) film, the d-spacing of $(0002)_{GaN}$ is slightly smaller than that of $(1\bar{1}0\bar{4})_{Al2O3}$, and is larger than that of $(0002)_{AlN}$, i.e., the GaN layer buffers the lattice mismatch between the AlN film and the Al_2O_3 substrate. The lattice mismatches of the AlN/GaN and the GaN/Al_2O_3 interfaces are estimated to be −2.6% and −0.3%, respectively.

3.2. Microstructures

3.2.1. Cross-sectional structures

Fig. 1 shows the $AlN(1\bar{1}00)$ cross-sectional bright-field TEM images. In the AlN/Al_2O_3(+4° off-cut) film and the $AlN/GaN/Al_2O_3$ (just-cut, −4° off-cut) films, cracks perpendicular to the interface between the films and the substrates are observed, as shown in Fig. 1a, c and d. The cracks do not propagate to the AlN film surface. The tips of the cracks are the widest in the AlN films, and the cracks narrow as they penetrate deeply into the substrates. The defects along the $(0001)_{AlN}$ plane do not propagate to the AlN film surfaces. On the other hand, in the $AlN/GaN/Al_2O_3$ (+4° off-cut) film, no cracks are observed and the defects along the $(0001)_{AlN}$ plane sometimes propagate to the AlN film surface, as shown in Fig. 1b. These TEM images indicate that the crystallinity in the AlN films depends on the planar imperfections, i.e., the low crystallinity in the $AlN/GaN/Al_2O_3$ (+4° off-cut) film is attributable to the propagated planar imperfections.

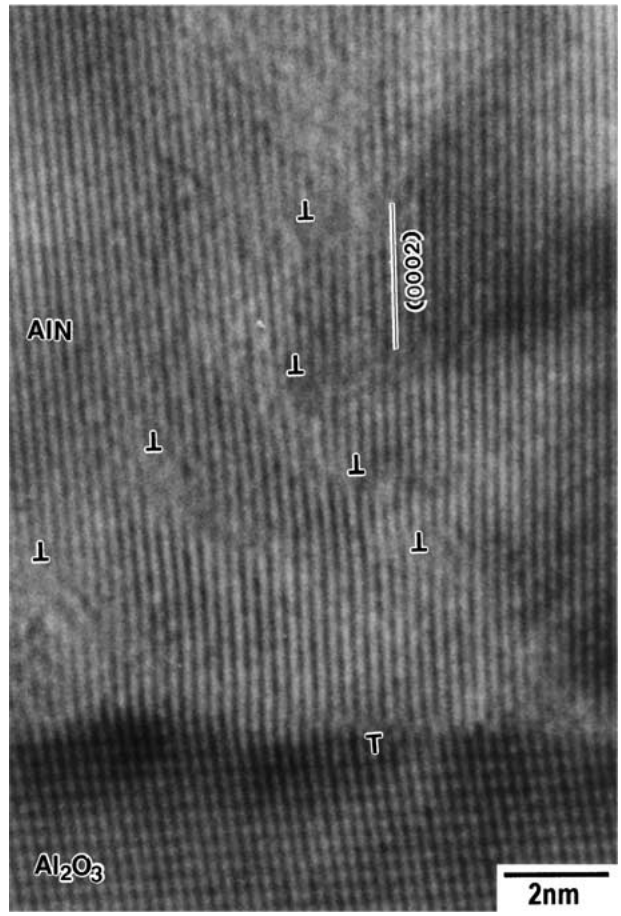

Figure 4 AlN $(1\bar{1}00)$ cross-sectional high-resolution TEM image of the AlN/Al_2O_3(+4° off-cut) interface. Misfit dislocations are labeled ⊥ or ⊤.

On the basis of these results, the cracking process in the $AlN/GaN/Al_2O_3$ (just-cut, −4° off-cut) films may be concluded to be the same as that in the AlN/Al_2O_3 (+4° off-cut) film, as we have reported in the previous study [12], i.e., the cracks are formed in the AlN film due to the tensile stress along the $[0001]_{AlN}$ direction during the epitaxial growth and simultaneously propagate to the AlN film surface and into the Al_2O_3 substrate. The tensile stress is induced by the annihilation of the defects along the $(0001)_{AlN}$ plane.

3.2.2. Interface structures

3.2.2.1. AlN/Al_2O_3 (+4° off-cut) film. Fig. 2 shows the cross-sectional TEM images of the AlN/Al_2O_3 (+4°

off-cut) film and the selected-area electron diffraction pattern in the vicinity of the interface. In the range from the interface to a film thickness of about 200 nm, the AlN/Al_2O_3 film exhibits a high density of lattice defects, and considerable moiré fringes with the spacing of about 3 nm and the extra electron diffraction spots other than those of the AlN epitaxial film and the Al_2O_3 substrate are observed. The spacing of the extra spot indicated by circles agrees with the moiré fringe spacing of 3 nm. A moiré fringe is formed from the overlap of two sets of planes with spacings d_1 and d_2; the moiré fringe spacing D is given as follows [15].

$$D = \left| \frac{d_1 d_2 \cos\phi}{d_1 - d_2} \right|$$

These overlapping planes meet at an angle of ϕ with each other. The d-spacing of $(0002)_{AlN}$ is 0.249 nm, and ϕ is 4° from the diffraction pattern. Therefore, the d_2-spacing of 0.271 nm is obtained by substituting 0.249 nm for d_1, 4° for ϕ and 3 nm for D.

Fig. 3 shows the cross-sectional high-resolution TEM images of the AlN/Al_2O_3 interface in the

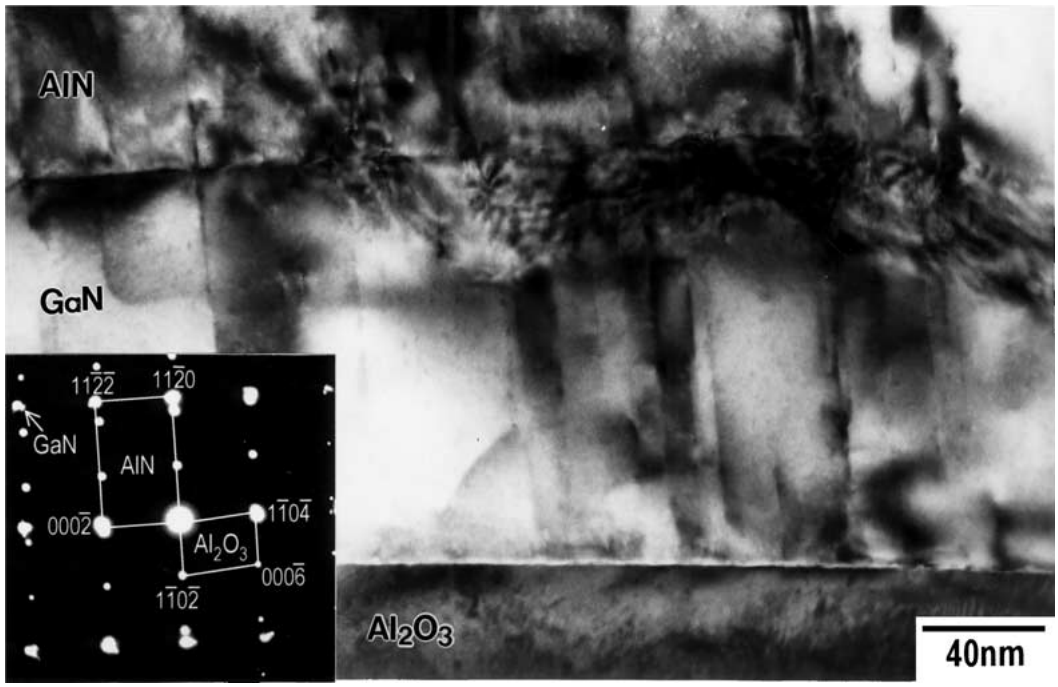

(a)

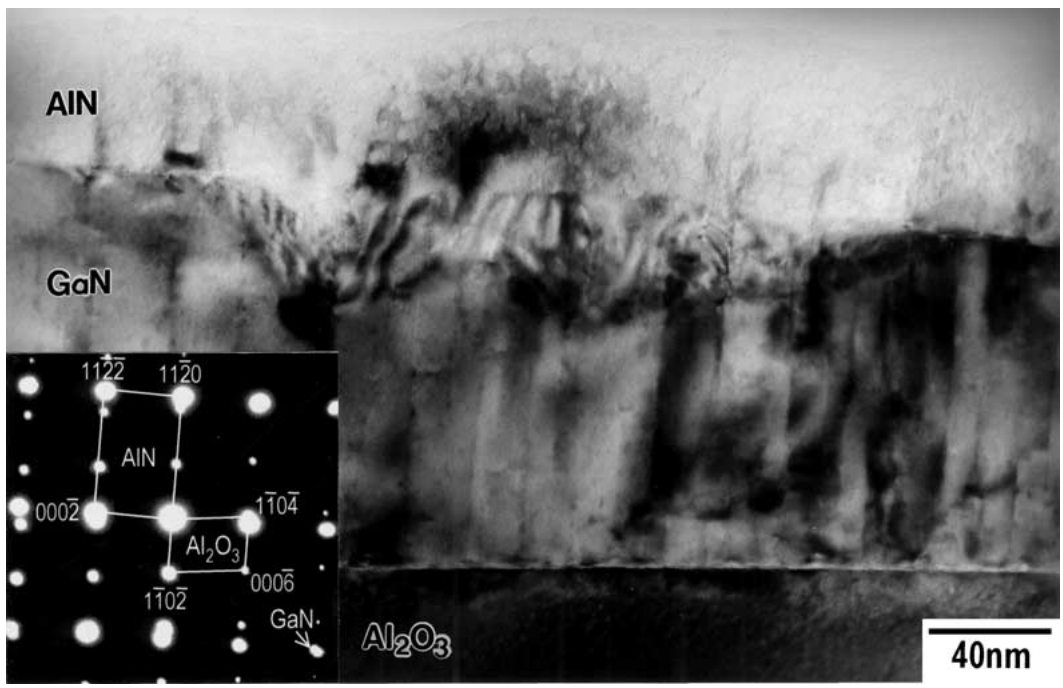

(b)

Figure 5 AlN $(1\bar{1}00)$ cross-sectional TEM images of (a) the AlN/GaN/Al_2O_3(+4° off-cut) film and (b) the AlN/GaN/Al_2O_3(−4° off-cut) film. Selected-area electron diffraction patterns at the bottom left of the micrographs were obtained in the vicinity of the AlN/GaN/Al_2O_3 interfaces.

AlN/Al_2O_3 film. The misfit dislocations labeled both $\perp$ and $\top$ are observed every 27–29 $(0002)_{AlN}$ planes on the left-hand side and right-hand side of Fig. 3a, respectively. Both distances between two misfit dislocations are about 7 nm, and the same numbers of misfit dislocations labeled $\perp$ and $\top$ are observed in an interval of at least 47 nm (corresponding to 182 $(0002)_{AlN}$ planes). According to the lattice constant measurements using HR-XRD, the lattice mismatch of the AlN/Al_2O_3 interface is estimated to be -2.8%. If it is assumed that the lattice mismatch is relaxed by edge dislocations, the edge dislocations labeled $\perp$ should be observed every 37 $(0002)_{AlN}$ planes at the interface. However, the high-resolution TEM images do not agree with the result of the lattice constant measurements. Although the mechanism of the occurrence of the dislocations labeled both $\perp$ and $\top$ is not clarified, the d-spacings of $(0002)_{AlN}$ in Fig. 3b and in c are estimated to be 0.247 nm and 0.265 nm, respectively. The d-spacing of 0.265 nm almost agrees with the d_2-spacing of 0.271 nm estimated using the above equation, so that it is suggested that the moiré fringe is caused by the overlap of these two sets. According to the high-resolution TEM image shown in Fig. 4, there is an edge dislocation labeled $\perp$ just above that labeled $\top$. In addition, several edge dislocations labeled $\perp$ are observed in the AlN film away from the interface. These TEM images indicate that the lattice mismatch between AlN and Al_2O_3 is relaxed in the AlN film. It can be stated that the generation of the edge dislocation labeled $\perp$ in the AlN film results in the change of the interplanar spacing from d_2 to d_1. Therefore, the moiré fringes disappear with increasing film thickness.

3.2.2.2. AlN/GaN/Al_2O_3 ($\pm4^\circ$ off-cut) film. Fig. 5 shows the cross-sectional TEM images of the $AlN/GaN/Al_2O_3(\pm4^\circ$ off-cut) films and selected-area electron diffraction patterns in the vicinity of the interfaces. The selected-area electron diffraction patterns show that $(11\bar{2}0)$-oriented AlN and GaN single crystals grow epitaxially on the $(1\bar{1}02)$ Al_2O_3 substrates. The density of lattice defects in the vicinity of the GaN/Al_2O_3 interfaces is low compared with the AlN/Al_2O_3 interface. The density of the lattice defects along the $(0001)_{GaN}$ plane in the GaN layer on the $+4^\circ$ off-cut substrate is lower than that on the -4° off-cut substrate, which supports the results of HR-XRD. The $AlN/GaN/Al_2O_3$ ($+4^\circ$ off-cut) film exhibits that

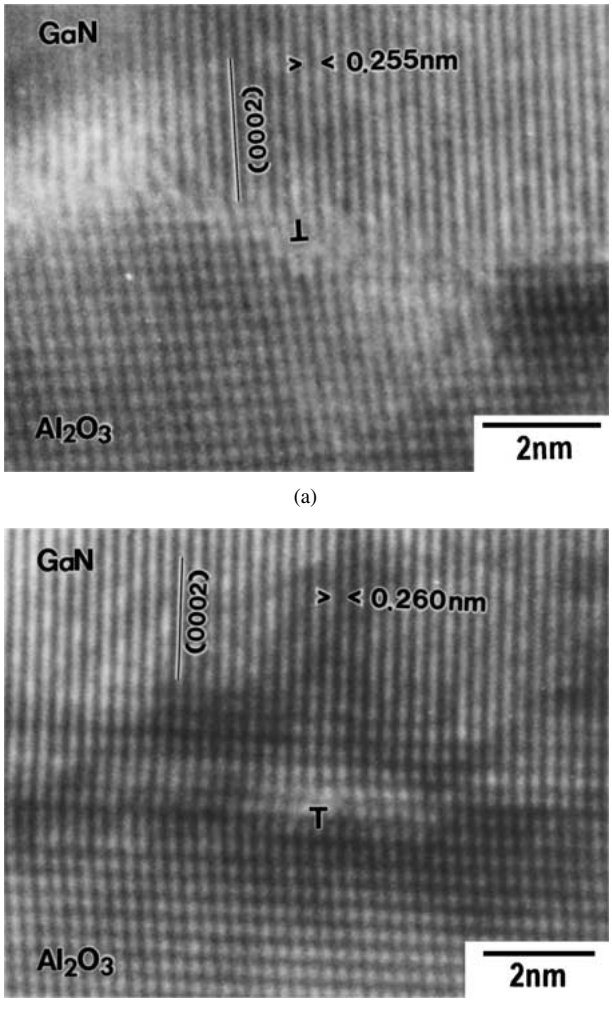

Figure 6 Cross-sectional high-resolution TEM images in the GaN/Al_2O_3 interfaces of (a) the $AlN/GaN/Al_2O_3(+4^\circ$ off-cut) film and (b) the $AlN/GaN/Al_2O_3(-4^\circ$ off-cut) film. Misfit dislocations are labeled $\perp$ or $\top$. Incident electron beam is parallel to $[1\bar{1}00]_{GaN}$// $[11\bar{2}0]_{Al2O3}$.

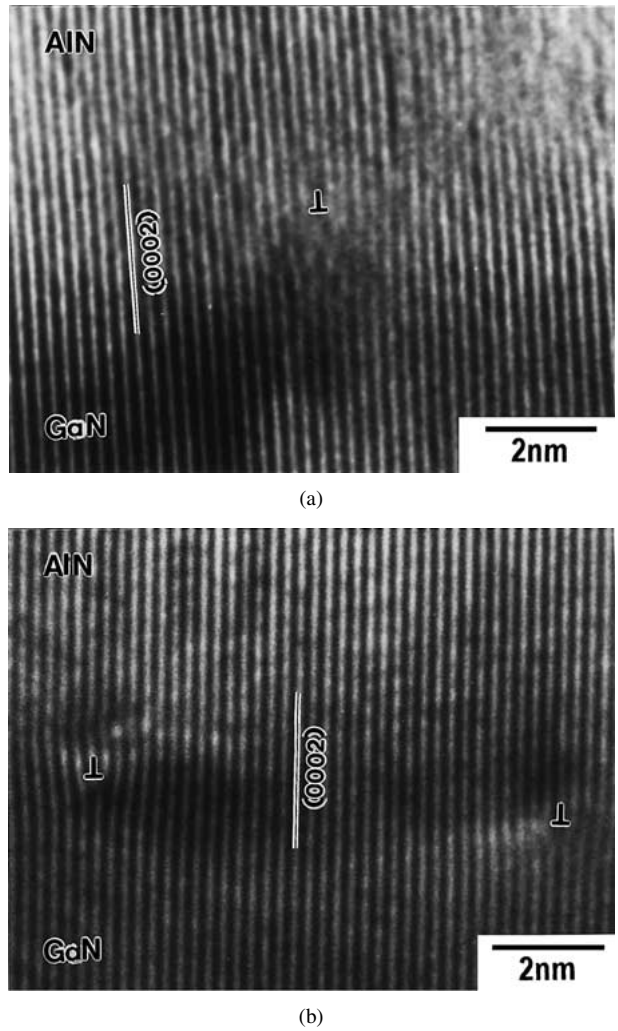

Figure 7 Cross-sectional high-resolution TEM images in the AlN/GaN interfaces of (a) the $AlN/GaN/Al_2O_3(+4^\circ$ off-cut) film and (b) the $AlN/GaN/Al_2O_3(-4^\circ$ off-cut) film. Misfit dislocations are labeled $\perp$. Incident electron beam is parallel to $[1\bar{1}00]_{AlN}$// $[1\bar{1}00]_{GaN}$.

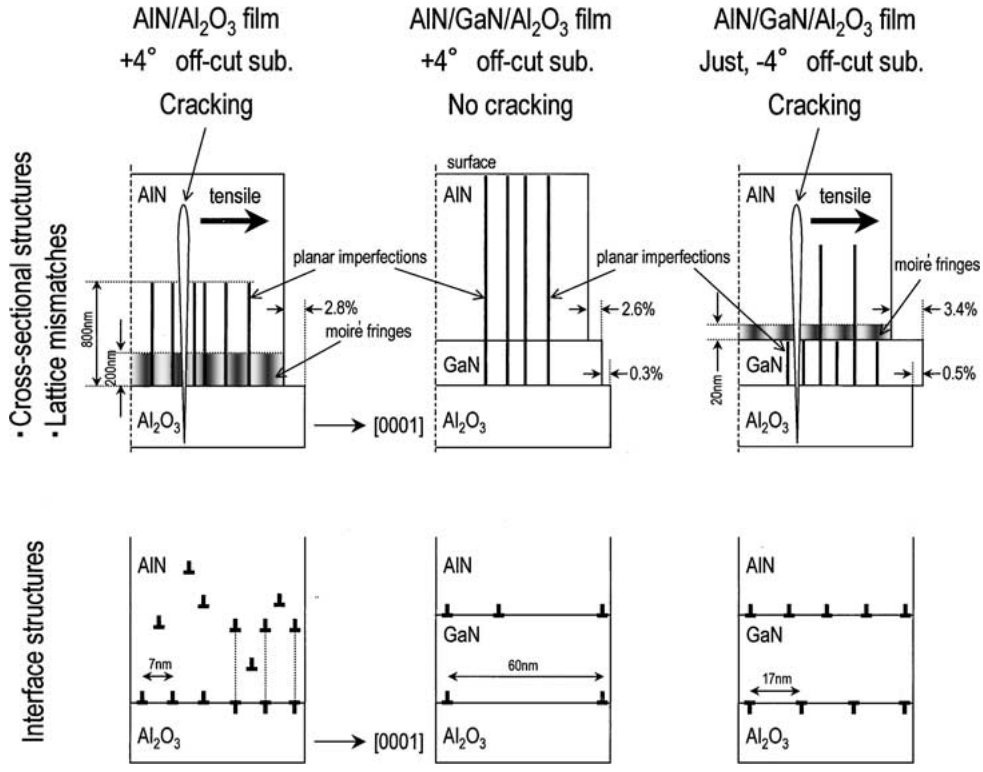

Figure 8 Schematic diagrams illustrating the relationship between the cross-sectional microstructures, the interface structures, the lattice mismatches and the cracking.

the lattice defects originating at the GaN/Al_2O_3 interface propagate into the AlN film, although strain contrasts are sometimes observed at the GaN side of the AlN/GaN interface. On the other hand, the AlN/GaN/Al_2O_3 (-4° off-cut) film sometimes exhibits moiré fringes about 20 nm thick at the AlN side of the AlN/GaN interface. The lattice defects along the $(0001)_{GaN}$ plane stop propagating at the interface where the moiré fringes are observed.

Fig. 6 shows the cross-sectional high-resolution TEM images of the GaN/Al_2O_3 interfaces in the AlN/GaN/Al_2O_3 ($\pm 4^\circ$ off-cut) films. The interfaces are sharp, and the lattice mismatches are relaxed by the edge dislocations. In the GaN/Al_2O_3 ($+4^\circ$ off-cut) interface, the misfit dislocations labeled $\perp$ are observed, and the lattice mismatch and the distance between two dislocations are estimated to be -0.4% and 60 nm, respectively. In the GaN/Al_2O_3 (-4° off-cut) interface, the misfit dislocations labeled $\top$ are observed, and the lattice mismatch and the distance between two dislocations are estimated to be $+1.6\%$ and 17 nm, respectively. Thus, these TEM images indicate that the d-spacing of $(0002)_{GaN}$ in the AlN/GaN/Al_2O_3 ($+4^\circ$ off-cut) film is smaller than that of $(1\bar{1}0\bar{4})_{Al2O3}$, whereas that in the AlN/GaN/Al_2O_3 (-4° off-cut) film is larger, which agree with the results of HR-XRD.

Fig. 7 shows the cross-sectional high-resolution TEM images of the AlN/GaN interfaces in the AlN/GaN/Al_2O_3($\pm 4^\circ$ off-cut) films. The misfit dislocations labeled $\perp$ are observed, although the dislocations can not be observed exactly because of the indistinct AlN/GaN interfaces. In the AlN/GaN/Al_2O_3 ($+4^\circ$ off-cut) and the AlN/GaN/Al_2O_3 (-4° off-cut) films, the lattice mismatches at the AlN/GaN interfaces are estimated to be -2.0% and -2.7%, respectively. Thus, these TEM images indicate that the lattice mismatch of the AlN/GaN interface in the AlN/GaN/Al_2O_3 ($+4^\circ$ off-cut) film is smaller than that in the AlN/GaN/Al_2O_3 (-4° off-cut) film, which agree with the results of HR-XRD.

3.3. Relationship between interface structures and cracking

Fig. 8 illustrates the relationship between the cross-sectional microstructures, the interface structures, the lattice mismatches and cracking. The AlN/Al_2O_3 and AlN/GaN interfaces in the AlN films with cracks (i.e. the AlN/Al_2O_3 ($+4^\circ$ off-cut) and the AlN/GaN/Al_2O_3 (just-cut, -4° off-cut) films) have low crystallinity and exhibit moiré fringes. The absolute lattice mismatches along the $[0001]_{AlN}$ direction of the interfaces are more than 2.8%. On the other hand, there are no moiré fringes in the vicinity of both the GaN/Al_2O_3 and the AlN/GaN interfaces in the AlN/GaN/Al_2O_3 ($+4^\circ$ off-cut) film without cracks. The absolute lattice mismatches are less than 2.6%, and the d-spacing along the [0001] direction decreases stepwise from the substrate to the AlN film via the GaN layer, i.e., the GaN layer buffers the lattice mismatch between the AlN film and the Al_2O_3 substrate. Therefore, it is concluded that the cracking in the AlN epitaxial films depends on the interface structures as follows. In the AlN/Al_2O_3 ($+4^\circ$ off-cut) film and the AlN/GaN/Al_2O_3 (just-cut, -4° off-cut) films, since the large lattice mismatches of the AlN/Al_2O_3 and AlN/GaN interfaces lead to the low crystallinity in the vicinity of the interface, the propagation of the lattice defects along the $(0001)_{AlN}$ plane is suppressed. As a consequence, the lattice defects are annihilated during the epitaxial growth, followed by the induction

of tensile stress along the $[0001]_{AlN}$ direction and the formation of the cracks. On the other hand, in the $AlN/GaN/Al_2O_3$ (+4° off-cut) film, since the buffering of the lattice mismatch between the AlN film and the Al_2O_3 substrate due to the GaN layer leads to the high crystallinity in the vicinity of the AlN/GaN interface, the lattice defects along the $(0001)_{AlN}$ plane can propagate to the AlN film surface. As a consequence, the tensile stress is suppressed and no cracks form.

4. Summary

The crystal structures and microstructures of the $AlN/GaN/Al_2O_3$ (just-cut, ±4° off-cut) films and AlN/Al_2O_3 (+4° off-cut) film grown by MOCVD were investigated.

(1) The AlN/Al_2O_3 (+4° off-cut) film and the $AlN/GaN/Al_2O_3$ (just-cut, −4° off-cut) films exhibited cracks parallel to the $[1\bar{1}00]_{AlN}$ direction and perpendicular to the interfaces of the films and the substrates, whereas the $AlN/GaN/Al_2O_3$ (+4° off-cut) film did not exhibit any cracks.

(2) In the AlN/Al_2O_3 (+4° off-cut) film and the $AlN/GaN/Al_2O_3$ (just-cut, −4° off-cut) films, the defects along the $(0001)_{AlN}$ plane did not propagate to the AlN film surfaces. In the $AlN/GaN/Al_2O_3$ (+4° off-cut) film, the defects sometimes propagated to the AlN film surface.

(3) The AlN/Al_2O_3 (+4° off-cut) film and the $AlN/GaN/Al_2O_3$ (just-cut, −4° off-cut) films exhibited moiré fringes in the vicinity of the AlN/Al_2O_3 and AlN/GaN interfaces. The absolute lattice mismatches of the interfaces along the $[0001]_{AlN}$ direction were 2.8% and 3.4%, respectively. The $AlN/GaN/Al_2O_3$ (+4° off-cut) film did not exhibit moiré fringes in the vicinity of both the GaN/Al_2O_3 and AlN/GaN interfaces, and the absolute lattice mismatches were 0.3% and 2.6%, respectively, The GaN layer buffered the lattice mismatch between the AlN film and Al_2O_3 substrate.

On the basis of these results, the effects of the interface structures on the cracking were discussed. The large lattice mismatches of the AlN/Al_2O_3 and the AlN/GaN interfaces in the AlN/Al_2O_3 (+4° off-cut) film and the $AlN/GaN/Al_2O_3$ (just-cut, −4° off-cut) films led to the low crystallinity interfaces and the annihilation of the lattice defects along the $(0001)_{AlN}$ plane. As a consequence, tensile stress was induced and cracks were formed in the AlN films during the epitaxial growth. On the other hand, in the $AlN/GaN/Al_2O_3$ (+4° off-cut) film, the lattice mismatch buffering due to the GaN layer led to the high crystallinity interfaces and the propagation of the lattice defects along the $(0001)_{AlN}$ plane. Therefore, tensile stress was suppressed and no cracks formed.

References

1. G. D. O'CLOCK, JR. and M. T. DUFFY, *Appl. Phys. Lett.* **23** (1973) 55.
2. M. T. DUFFY, C. C. WANG, G. D. O'CLOCK, JR., S. H. MCFARLANE III and P. J. ZANZUCCHI, *J. Electron. Mater.* **2** (1973) 359.
3. W. M. YIM, E. J. STOFKO, P. J. ZANZUCCHI, J. I. PANKOVE, M. ETTENBERG and S. L. GILBERT, *J. Appl. Phys.* **44** (1973) 292.
4. J. K. LIU, R. B. STOKES and K. M. LAKIN, in Proceedings of the 1975 IEEE Ultrasonic. Symp. (1975) p. 234.
5. K. TSUBOUCHI and N. MIKOSHIBA, *IEEE Trans. Sonics Ultrason.* **SU-32** (1985) 634.
6. T. SHIBATA, Y. HORI, K. ASAI, Y. NAKAMURA, M. TANAKA, K. KAIGAWA, J. SHIBATA and H. SAKAI, in Proceedings of the International Workshop on Nitride Semiconductors, IPAP Conf. Series 1 (2000) p. 981.
7. T. MATSUMOTO and M. AOKI, *Jpn. J. Appl. Phys.* **13** (1974) 1583.
8. N. ITOH, J. C. RHEE, T. KAWABATA and S. KOIKE, *J. Appl. Phys.* **58** (1985) 1828.
9. K. HIRAMATSU, T. DETCHPROHM and I. AKASAKI, *Jpn. J. Appl. Phys.* **32** (1993) 1528.
10. H. AMANO, M. IWAYA, T. KASHIMA, M. KATSURAGAWA, I. AKASAKI, J. HAN, S. HEARNE, J. A. FLORO, E. CHASON and J. FIGIEL, *ibid.* **37** (1998) L1540.
11. A. V. DOBRYNIN, *J. Appl. Phys.* **85** (1999) 1876.
12. K. KAIGAWA, T. SHIBATA, Y. NAKAMURA, K. ASAI, M. TANAKA, H. SAKAI and T. TSURUMI, *J. Mater. Sci.* **36** (2001) 4649.
13. W. J. BARTELS, *J. Vac. Sci. Technol.* **B1** (1983) 338.
14. P. F. FEWSTER and N. L. ANDREW, *J. Appl. Crystallogr.* **28** (1995) 451.
15. P. B. HIRSH, A. HOWIE, R. B. NICHOLSON, D. W. PASHLEY and M. J. WHELAN, in "Electron Microscopy of Thin Crystals" (London Butterworths, London, 1965) p. 357.

Received 7 March
and accepted 21 November 2001